nce less than 3 Å which is sum of the van der Waals radius of oxygen. These hydrogen bonds formed through water molecules interconnect the two parallel layers of sodium tris (oxalato) chromate unit separated by *c*/2 and may stabilize the molecular packing.

These two Mg^{2+} ions will create two different ligand field enviroment for the $Cr(ox)_3^{3-}$ and may cause the small (2-3 cm^{-1}) splitting in optical spectrum. One may suggest the possibility of this splitting as zero field splitting. However, EPR study suggested the magnitude of zero field splitting as 0.9 cm^{-1}. Mortensen suggested that this optical splitting is due to exchange interaction between separate $Cr(ox)_3^{3-}$ ions.[2] But it is very unlikely since the closest Cr-Cr separation is determined as 8.282 Å and the same splitting is observed in 1-5% $Cr(ox)_3^{3-}$ doped in NaMg salt of $Al(ox)_3^{3-}$ complex where the separation of Cr-Cr is even expected to be larger.

Acknowledgement. This work was supported by Non-directed Research Fund, Korea Research Foundation. I.-H. Suh thanks the Korean Science and Engineering Foundation for the support.

References

1. Condrate, R. A.; Forster, L. S. O. *J. Mol. Spectros.* **1967**, *24*, 490.
2. Mortensen, O. S. *J. Chem. Phys.* **1967**, *47*, 4215.
3. Coleman, W. F. Coleman, *J. Lumin.* **1975**, *10*, 163.
4. Berheim, R. A.; Reichenbecher, E. F. *J. Chem. Phys.* **1969**, *51*, 996.
5. Coleman, W. F. *J. Lumin.* **1980**, *22*, 17.
6. Schönherr, T.; Spanier, J.; Schmidtke, H.-H. *J. Phys. Chem.* **1989**, *93*, 5969.
7. Hoggard, P. E.; *Coord. Chem. Rev.* **1986**, *70*, 85.
8. Bailar, J. C.; Jones, E. M. *Inorg. Synthesis.* **1939**, *1*, 35.
9. Gmelines handbuch der Anorganische Chemie, *System 52 (Chromium)*, Teil B, **1962**, 791.
10. Suh, I. H.; Choo, G. H.; Lee, J. H.; Lim, S. S.; Ryu, B. Y. *Chungnam J. Sci.* **1992**, *19*, 87.
11. Suh, I. H.; Kim, K. J.; Choo, G. H.; Lee, J. H.; Choh, S. H.; Kim, M. J. *Acta Cryst.* **1993**, *A49*, 369.
12. Sheldrick, G. M. SHELX-86, Univ. Goettingen, Federal Republic of Germany.
13. Sheldrick, G. M. SHELX-76, *A program for Crystal Structure Determination*, Univ. of Cambridge, England **1976**.
14. Peterse, W. J. A. M.; Plam, J. H. *Acta Cryst.* **1966**, *20*, 147.
15. Taylor, D. *Aust. J. Chem.* **1978**, *31*, 1455.
16. Ambady, G. K.; Kartha, G. *Acta Cryst.* **1968**, *B24*, 1540.
17. Johnson, C. K. *Acta Cryst.* **1965**, *18*, 1004.

Time-resolved UV Fluorescence Spectroscopy of Aorta and its Related Chromophores, Collagen and Elastin, Using 320 nm Excitation

Young D. Park

Department of Chemistry Ajou University, Suwon 441-749
Received December 24, 1993

Fluorescence time decay of human aorta has been measured at 380, 440, 480 nm using 320 nm excitation and time-correlated single photon counting technique. Fluorescence decay was found to be nonexponential at all emission frequencies. The normal and diseased sample showed significantly different fluorescence behaviors at 380 nm while this time decay difference was decreased in the fluorescence at 440 and 480 nms. The decay data were multiexponential and were analyzed with two exponential decay constants. The fluorescence decays were compared with and analyzed in terms of collagen and elastin.

Introduction

Laser-induced fluorescence (LIF) spectroscopy has proved to be one of the most sensitive detection methods and has become a powerful tool in the field of analytical chemistry. LIF spectroscopy has been widely used in biology and medicine and more recently in the characterization of human tissue.[1-4] The study of arterial wall spectroscopy, in particular, has drawn considerable interest because atherosclerosis account for a large proportion of heart attacks and cases of ischemic heart disease[5]. Atherosclerosis also accounts for many strokes, numerous instances of peripheral disease, most aneurysms of the lower abdminal aorta, which can rupture and cause sudden fatal hemorrhage[6]. Laser induced fluorescence has great potential for arterial wall diagnosis due to its sensitivety, and its ability to be monitored remotely using optical fiber probe. Since fluorescence emission is affected by the fluorophors constitution and their surrounding environments, normal and diseased plaque tissue are expected to yield different fluorescence behavior both in frequency and time domain. In this paper, we would like to focus our discussion on the time resolved study of aorta fluorescence spectroscopy.

Aorta is a large elastic artery and is made of three major microscopic layers: the intima, the media, and the adventitia[6]. These layers are separated by elastic sheets. The intima is

the innermost layer and consists of a luminal layer of thin endothelial cells and the subendothelial connective tissue. The endothelium is a monolayer of cells 0.1-3 μm thick, and it sits on a 50 nm thick basement membrane (basal lamina) of loose collagen microfibrils intermixed with various proteoglycans. The remainder of the intima, the subendothelial connective tissue matrix, consists of collagen fibers, and ground substance. Typical intimal thickness of normal aorta is about 100-200 μm. The middle layer, the media, typically about 500 mm thick, consists of 40-70 concentric elastic lamellae 5-15 μm apart and 2-3 μm thick[7]. Sheets of helically arranged smooth muscle separate these lamellae. A thin, discontinuous basement membrane surrounds each smooth muscle cell, and variable amounts of collagen, elastin, and ground substance fill the small interstitial space between smooth muscle cells and the elastic sheets. The media is the primarily load-bearing layer. The adventitia is the outmost layer is composed of fairly disoranized collection of connective tissue, scattered fibroblasts and smooth muscle cells, and adipose tissue. The advantitia does not play any significant role in the case of aorta fluorescence spectroscopy due to its distance from intimal surface.

There have been numerous studies in the arterial vessel LIF spectroscopy to identify and characterize athrosclerotic plaques[1-3]. These studies have been successful in the indentification of diseased tissue using experimental fluorescence lineshape and fitting it to a model incorporating fluorescence spectra of different chromophores present in the tissue[2,3]. Most of these studies so far used conventional frequency domain spectroscopy. In this domain, one usually monitors the light-tissue interaction using an appropriate laser for excitation and dispersing the fluorescence.

With the advent of ultrashort pulsed lasers, time domain fluorescence spectroscopy of biomolecules has become prevalent[8]. The fluorescence decay of a system is examined 1) to deconvolve chromophore within a system and/or 2) to study the influence of environment on a particular chromophore. Fluorescence decay of some chromophores has been used to study its environment because of its sensitivity to its neighbors. Trytophan is one of the biomolecules whose fluorescence decay has been intensively used to study protein structure and dynamics[9,10]. In previous work, we have studied the fluorescence decay of tryptophan in arterial tissue using 287 nm and we observed no significant differences in temporal behavior of tryptophan fluorescence for normal and diseased aorta. The fluorescence decay was highly non-exponential[3].

In this paper, we address the fluorescence decay of aorta and its fluorophors using 320 nm excitation. At this excitation frequency, fluorophores associated with collagen and elastin has been shown to be the major contributions to the fluorescence in aorta[11]. Fluorescence decay was monitored at 380, 440 and 480 nm for narmal and atherosclerotic aorta samples.

Experimental

Figure 1 shows the experimental apparatus including the picosecond dye laser system and time-correlated single photon counting (TCSPC) system assembled at the Spectroscopy Laboratory for studies in the biomedical and physical sciences. The second harmonic of mode-locked Nd : YAG laser (Coherent Antares 76-S, at 532 nm, 70 ps FWHM, 76 MHz, average power 1.5 W) pumps a cavity-extended Coherent 590 dye laser synchronously. The repetition rate of the dye laser was reduced to 1 MHz using a cavity dumper to enable data aquisition using TCSPC. The output of the dye laser had a 5 ps pulse width. The tissue samples were excited by frequency-doubling the dye laser with a nonlinear crystal ($LiIO_3$) and reducing energy to 1 pJ/pulse to minimize UV exposure-induced spectral changes in the tissue. Total fluence for a given sample was not greater than 10 mJ mm^{-2}. Both the excitation and fluorescence collection was executed using a fiber system consisting of one 200 micron core center fiber surrounded with 6 other fibers. The center fiber was used for delivery of excitation laser and the surrounding ones were for fluorescence collection. This device is particularly useful for the study of tissue because of its accuracy in the position of illuminated area, ability to fluorescence from only selected illuminated area and easy handling. The fluorescence excited by the UV laser and collected by fiber device were focused into a 0.2 m monochromator (Instrument SA HR-20). A 345 nm long-pass filter (WG-345, Schott Filter) was placed before the monochromater entrance to eliminate scattered laser light. The dispersed fluorescence was detected by a MCP PMT (Hamamatsu 1564-U-07, 90 psec transit time spread), and the time difference between this signal and a reference signal from a photodiode was converted into a voltage by a time-to-amplitude converter (TAC Canberra 2143), and stored into a personal computer via a multichannel analyzer (Nucleus PCA). The data was then sent to and analyzed by a SUN SPARC-10 workstation. The photon counts was maintained less than 3 percent of the repitition rate to minimize any potential photon pile-up complications[11]. The overall system response time was measures as 130 ps (FWHM). The fluorescence decay curves were fit with multiexponential decay parameters by the method of iterative convolution[11]. The quality of the fit was judged by the χ^2 criterion and by visual inspection of the weighted residuals.

Human aorta specimens were obtained at the time of post-

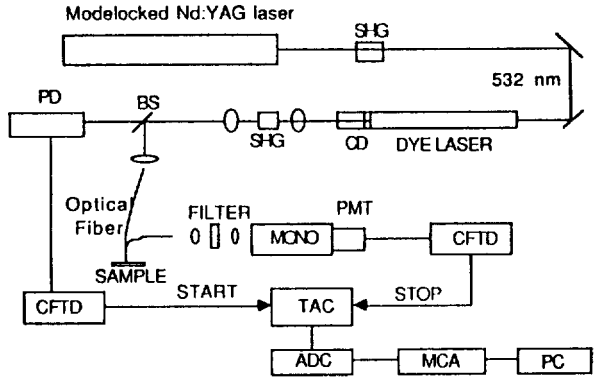

Figure 1. Experimental apparatus used in this study. Abbriviations: CD=cavity dumper; SHG=second harmonic generating crystal; BS=beam splitting mirror; PD=photodiode; MONO=monochromator; PMT=microchannel plate photomultiplier; CFTD=constant fraction timing discriminator; TAC=time-to-ampitude converter; ADC=anaolog digital converter; MCA=multichannel analyzer; PC=personal computer.

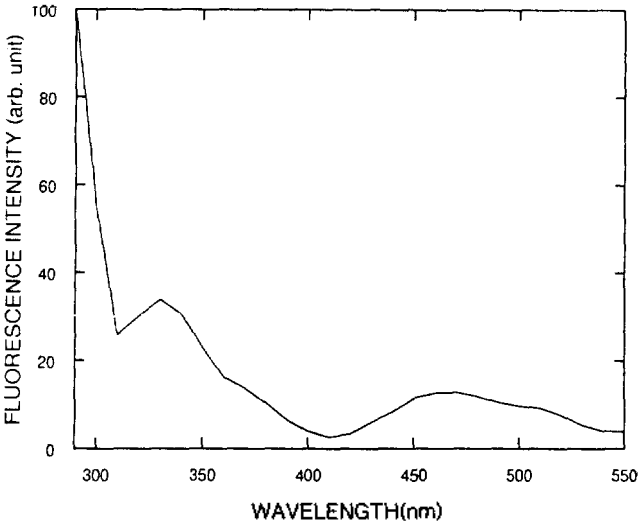

Figure 2. Fluorescence excitation spectrum of normal aorta. The fluorescence at each wavelength was collected up to 700 nm.

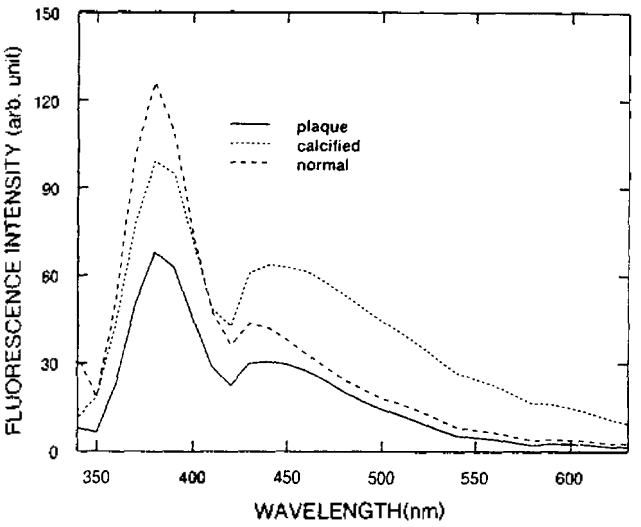

Figure 3. Steady state fluorescene spectra of normal and diseased aorta when excited at 320 nm. Spectra were taken using SPEX fluorog.

mortem examination and were snap frozen in isopentane and liquid nitrogen and stored at −70℃ until use. Samples were brought to room temperature and kept moist with pH 7.4 buffered saline immediately prior to spectroscopic examination. Tissue samples studied in this experiment were sent for pathology at Cleverand Clinic Foundation at Cleverand, OH. A total of sixteen normal, ten non-calcified and ten calcified plaque samples was studied.

For the study of pure collagens and elastin, the samples were obtained from Sigma Chemical Co. and were used without further purification. Three kinds of type I collagens (Sigma types I, II, V from bovine achilles tendon) and an elastin (Sigma, from bovine neck ligament), were utilizen in this experiment.

Results and Discussion

Fluorescence of aorta. Figure 2 shows the fluorescence exciation spectrum of normal aorta. At each excitation wavelength, the fluorescence was taken by integrating all fluorescence ranging from 20 nm below excitation frequency up to 700 nm using SPEX fluorog. There are three major spectral bands appear in the excitation spectum. The band below 310 nm is primarily due to the fluorescence of amino acid tryptophan in tissue protein. The band peaks around 330 and 470 nm is due to the fluorescence of collagen and elastin. The valley of 415 nm is due to absorption of hemoglobin from lysed red blood cells in the tissue sample.

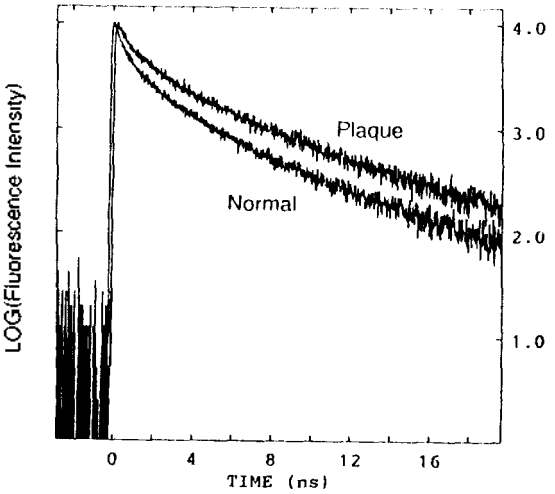

Figure 4. Fluorescence decay of normal and plaque (non-clacified) aorta at 380 nm when excited at 320 nm.

Figure 3 shows typical steady state fluorescence spectra of normal and diseased aorta samples when excited at 320 nm. At this excitation wavelength, the fluorescence spectrum is dominated by a prominent peak at near 380 nm with a smaller broad side band centering near 440 nm. Baraga and coworkers studied the fluorescence behavior using tunable UV pulsed dye laser and concluded that those two bands are due to hemglobin that they are both due to collagen and elastin. The band at 380 nm is due to the fluorescence from collagen and elastin in the aorta sample. The band centered near 440 nm is a distorted spectrum of fluorescernce from collagen and elastin by hemoglobin absorption[4].

Fluorescence decay of aorta. The fluorescence decay of aorta was examined at 380, 440, and 480 nm using 320 nm excitation. Figure 4 shows typical fluorescence decay curves of normal and plaque sample at 380 nm. The decay of aorta is highly non-exponential indicating the complexity of tissue chromophore environment. It was necessary to use at least three or four time constants for an appropriate fit of the data using multiexponential methods. A fit to four exponential decay constants requires very large signal to noise ratio. This was unfortunately not possible in the present experiments to avoid physical and spectroscopic changes in tissue due to radiation overexposure to the tissue. Therefore the analysis was carried out for the best fit with two decay time constants. Figure 5 shows the quality of the two exponential for typical aorta fluorescence. As we can see from the figure, the quality of the fit was not good, indicating that fluorescence decay of the aorta system is more complex than two exponential decay. When we fit the decay with

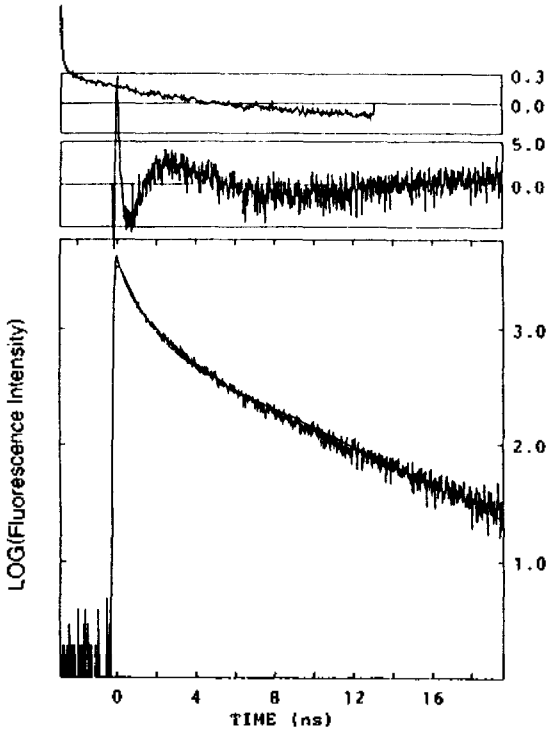

Figure 5. Quality of two exponential fit for a 380 nm normal aorta decay. Fitted decay curve is overlayed with experimental curve. The curve above the decay curve is the residuals of the fit, and the top curve is autocorrelation of the residuals. The fitted results for the figure is 0.78 exp($-t$/0.85(ns))+0.22 exp ($-t$/5.24(ns)), and χ^2=3.2.

two decay time constants, we get a fast (t_1) and a slow (t_2) time constants with their respective preexponentials (A_1 and A_2).

Figure 6 shows the fit results at 380 nm. As can be seen from the figure, A_1, the preexponential coefficient for fast decay constant of normal tissue is larger and less distributed than that of non-calcified plaque. The average of A_1 for calcified plaque is similar to that of normal, yet calcified plaque sample shows much wider distribution indicating that calcified samples are widely variable. The fluorescence decay analysis resulted very good separation between normal and non-calcified plaque for all fitting parameters, and $\langle t \rangle$, the average decay time, which is defined as $A_1t_1+A_2t_2$, was the best parameter for separation of normal and non-calcified plaque.

Figure 7 shows the fit results of fluorescence decay at 440, and 480 nm. Fluorescence decays at 440 and 480 nm, contrary to 380 nm decay, show little separation between different tissue types. Baraga and others[12] already showed that fluorescence of aorta at 380 when excited by a UV light originates from collagens and elastins. They also found that collagen and elastin fluorescence peak at 380 nm. The total fluorescence intensity decreases more rapidly than that of elastin as wavelength moves away from 380 nm to higher. The results are summarized in the table below (Table 1).

As we can see from the decay curve and the analysis, there is significant difference between normal and plaque samples for decay at 380 nm emission. Normal samples de-

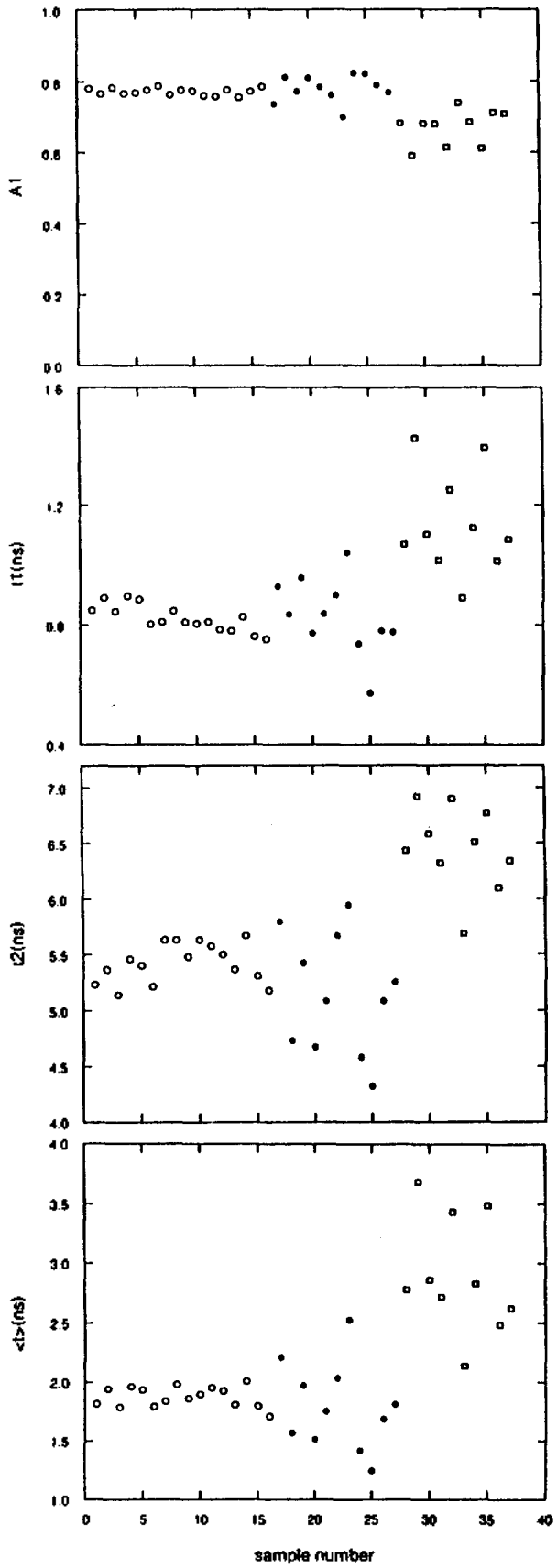

Figure 6. Fit results of fluorescence decay of aorta at 380 nm when excited at 320 nm.

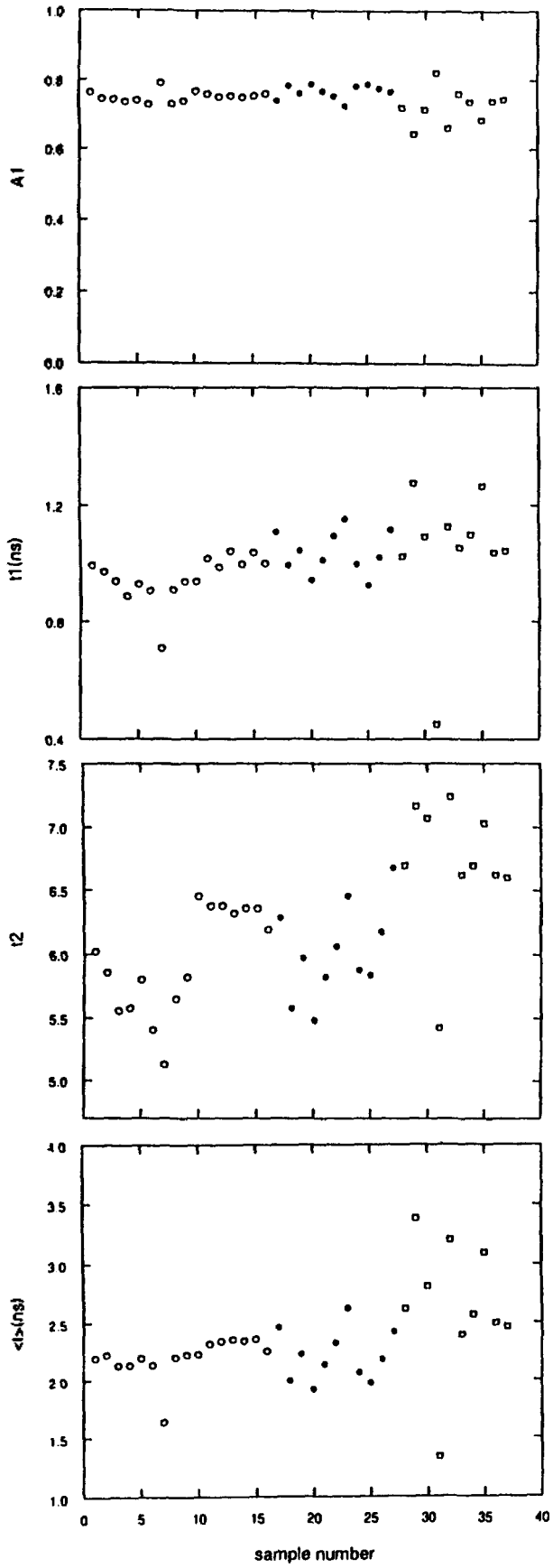

Figure 7. Fit results of fluorescence decay of aorta at 440 nm when excited at 320 nm.

Table 1. Two-exponents fit results of fluorescence decay of human aorta when excited at 320 nm and monitored at (a) 380, (b) 440 and (c) 480 nm

(a) for 380 nm emission

	A_1	A_2	t_1(ns)	t_2(ns)	$\langle t \rangle$
normal	0.77± 0.01	0.23± 0.01	0.88± 0.04	5.4± 0.2	1.87± 0.08
calcific	0.78± 0.04	0.22± 0.04	0.83± 0.12	5.1± 0.5	1.80± 0.36
plaque	0.67± 0.05	0.33± 0.05	1.14± 0.16	6.5± 0.4	2.90± 0.46

(b) for 440 nm emission

	A_1	A_2	t_1(ns)	t_2(ns)	$\langle t \rangle$
normal	0.75± 0.02	0.25± 0.02	0.95± 0.08	6.0± 0.4	2.20± 0.17
calcific	0.76± 0.02	0.24± 0.04	1.04± 0.07	6.0± 0.3	2.21± 0.21
plaque	0.72± 0.05	0.28± 0.05	1.05± 0.22	6.7± 0.5	2.63± 0.54

(c) for 480 nm emission

	A_1	A_2	t_1(ns)	t_2(ns)	$\langle t \rangle$
normal	0.72± 0.03	0.28± 0.03	0.98± 0.12	5.7± 0.6	2.33± 0.27
calcific	0.74± 0.01	0.26± 0.01	1.20± 0.09	6.6± 0.4	2.58± 0.17
plaque	0.74± 0.05	0.26± 0.05	1.00± 0.22	6.5± 0.7	2.46± 0.53

*A and t are preexponential coefficient and decay time, respectively.

cay faster than the plaques. In an analysis based on two exponential constants, normal tissue samples gave to 0.88 and 5.4 ns, while the plaque sample gave to 1.14 and 6.5 ns. The amount of fluorescence in each decay time also varies showing that plaque samples have more fluorescence yield with longer time constants. The fluorescence decay at 440 and 480 nm showed much smaller difference between normal and plaque arota.

Measurement of fluorescence decay rate can be used to determine the fluorescence quantum yield of a system. The fluorescence quantum yield is the ratio of fluorescence lifetime to the radiation lifetime of the chromophore. The measured decay rate of the aorta tissue is about 1.8 to 2.5 ns and the radiation lifetime of a typical molecular system is in the order of 10 to 100 nsec, the fluorescence quantum yield of the aorta chromophore at 320 nm is in the order of few percent. However, the fluorescence quantum yield of aorta chromophore is not the fluorescence quantum yield of aorta because aorta is optically thick.

Fluorescence decay of collagens and elastin. As we mentioned above, mentioned above, collagen and elastin are among the fluorophores responsible for this emission. To understand more about the nature of collagens and elastin and their behavior in the tissue, we have undertaken time resolved fluorescence spectra of pure samples of these compounds for comparison and analysis (Fig. 9).

Collagens used in the experiment are type I collagens from bovine achilles tendon and elastin is from bovine neck ligamant. The two time constants fit results of the fluorescence decay are shown in Table 2. The results indicate that fluorescence of elastin decays faster then that of collagens at all emission wavelenths with excited at 320 nm. The differences between decay time of collagen and elastin is greatest at

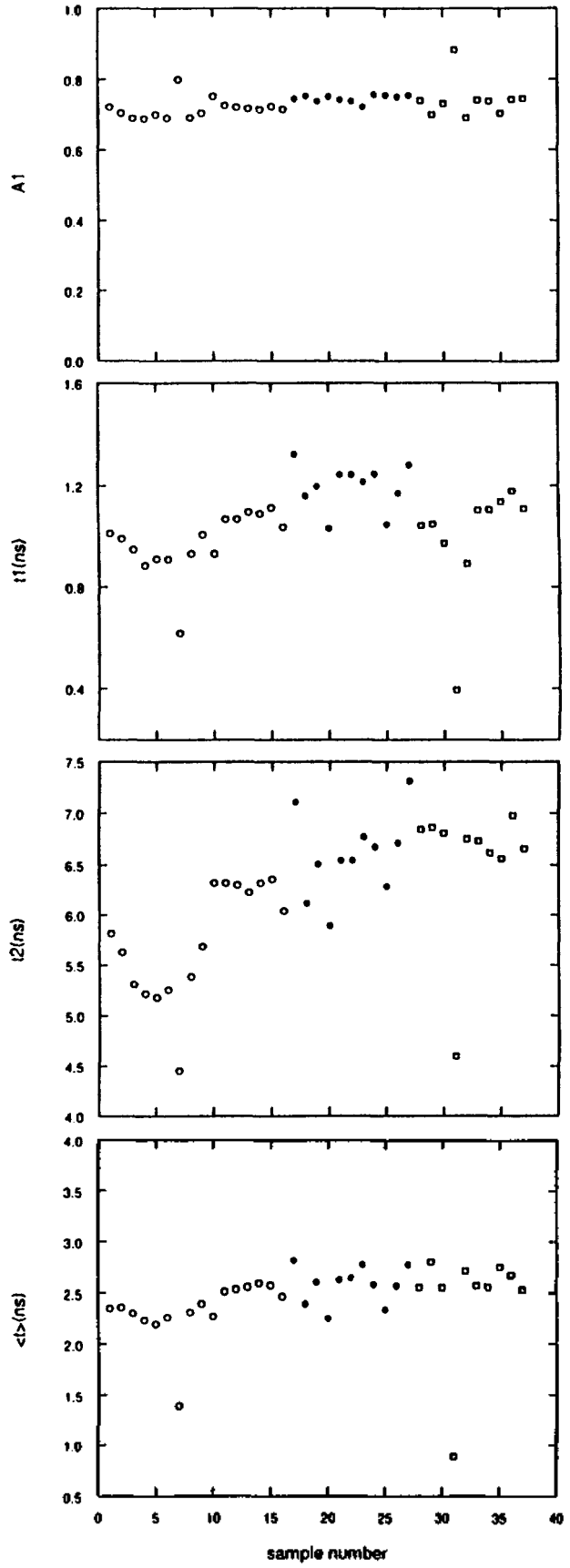

Figure 8. Fit results of fluorescence decay of aorta at 480 nm when excited at 320 nm.

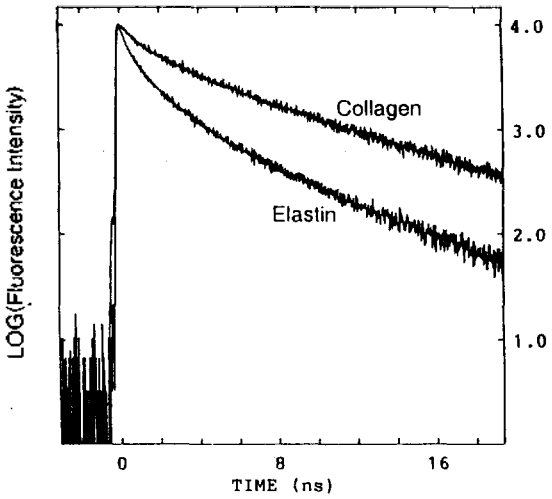

Figure 9. Fluorescence decay of collagen and elastin. Fluorescence was excited at 320 nm and monitored at 380 nm. Powered collagen type I from bovine achilles tendon and elastin from bovine neck ligament was used.

Table 2. Fluorescence decay of collagens and elastin. Samples were excited at 320 nm and fluorescence were monitored at (a) 380 nm, (b) 440 nm, and (c) 480 nm. All data were taken with dry powder sample

(a) 380 nm emission

	A_1	A_2	t_1(ns)	t_2(ns)	$\langle t \rangle$
collagen I*	0.53	0.47	1.47	7.36	4.22
collagen I**	0.56	0.44	1.40	7.39	4.03
collagen I***	0.47	0.53	1.42	7.79	4.80
elastin****	0.79	0.21	0.86	4.92	1.72

(b) 440 nm emission

	A_1	A_2	t_1(ns)	t_2(ns)	$\langle t \rangle$
collagen I*	0.59	0.41	1.37	8.11	4.14
collagen I**	0.60	0.40	1.49	8.21	4.19
collagen I***	0.51	0.49	1.33	8.19	4.66
elastin****	0.72	0.28	1.35	6.86	2.89

(c) 480 nm emission

	A_1	A_2	t_1(ns)	t_2(ns)	$\langle t \rangle$
collagen I*	0.63	0.37	1.45	8.45	4.03
collagen I**	0.62	0.38	1.59	8.50	4.21
collagen I***	0.56	0.44	1.38	8.40	4.49
elastin****	0.67	0.33	1.63	7.64	3.62

*from bovine achilles tendon (Sigma type I), **from bovine achilles tendon (Sigma type II), ***from bovine achilles tendon (Sigma type V), ****from bovine achilles tendon (Sigma).

380 nm. If the fluorescence of the tissue is mainly due to only collagens and elastin, the those sample containg more relative concentration would exhibit slower decay behavior, and the difference would be greatest when the difference

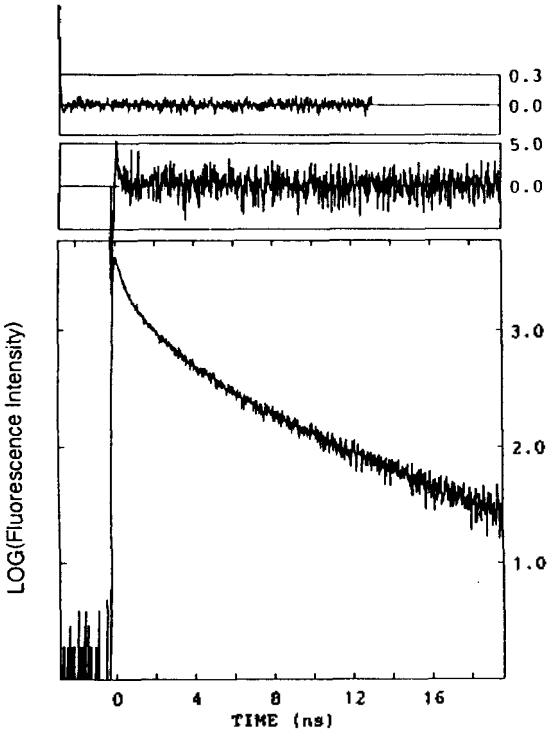

Figure 10. Quality of the fit of aorta decay using Eqn. 1. Residuals and its correlations were shown on top of the decay curve. The fit curve is not shown because there is no visible difference between data and fitted curve.

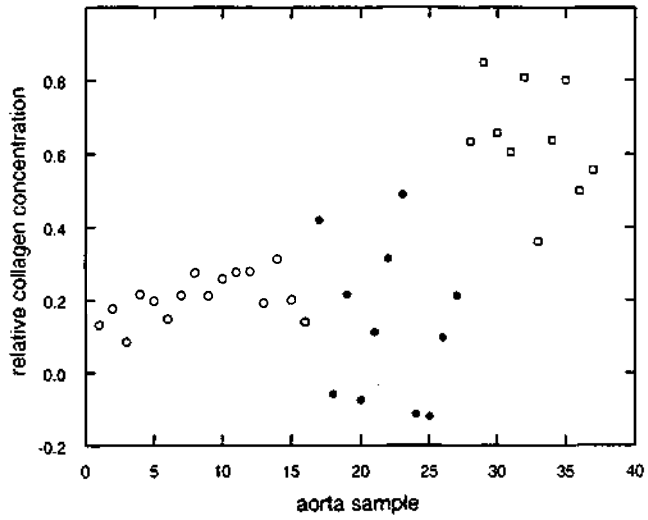

Figure 11. Fit result of arota fluorescence decay at 380 nm using collagen and elastin fluorescence decay as $F1(t)$ and $F2(t)$ in Equation 1.

in the decay time between collagen and elastin is greatest. This result explains why plaque sample, which has thicker collagen layer than normal tissue, has slower decay and the difference between normal and plaque is greatest at 380 nm.

Collagen and Elastin decay as a basis set for aorta fluorescence decay. As was mentioned above, tissue fluorescence decay at 380 nm shows significant difference between normal and plaques. If the fluorescence at 380 nm are mainly coming from collagen and elastin, we can approximate the fluorescence decay, $F(t)$, as the sum of its fluorophores, *i.e.*

$$F(t)=c1\ F1(t)+c2\ F2(t) \quad (1)$$

where $c1$ and $c2$ are concentration of collagen and elastin, respectively, and $F1(t)$ and $F2(t)$ are the decays of collagen and elastin, respectively. Note the simplicity of the equation and that there is no effect of absorber in this equation. This approach is an excellent approximation if there is no energy transfer between collagen and elastin and collagen and elastin are only fluorophores in the system. $F1(t)$ and $F2(t)$ were tried as the experimental data obtained using powdered collagen and elastin as a first approximation. As is shown in Figure 10, the fit is remarkablely good in spite of the crude basis set used for collagen and elastin decay. The coefficient $c1$ and $c2$ can be as fluorophor concentrations. Figure 11 shows the results of normalized $c1$ $(=c1/(c1+c2))$ using Eq. (1). This normalized $c1$ can be interpreted as relative concentration of collagen content in aorta fluorescence. As one can find from the figure, normal aorta shows much smaller $c1$ than that of plaque. Again, calcified plaque shows wider distribution of this value.

Conclusion

The fluorescence time decays of aorta samples and its fluorophores collagen and elastin at 380 nm, 440 nm and 480 nm were studied using excitation wavelength of 320 nm. The normal and diseased aorta samples showed significant different fluorescence decay behaviors at 380 nm, while this decay difference was decreased in the fluorescence at 440 and 480 nm. The data was analyzed with two exponential decay constants. The fluorescence decay were further analyzed in terms of its fluorophores; collagen and elastin. The result was consistant with tissue composition. The time-resolved spectroscopy of tissue can yield information on physical processes and chemical environment and is complementary to studies in frequency domain spectroscopy.

Acknowledgement. Most of the experimental work has been done at the Harrison Spectroscopy Laboratory at MIT. The author would like to thank to Dr. R. Dasari and Prof. M. S. Feld at MIT for their support. Dr. M. Fitzmaurice is also acknowledged for tissue pathological analysis. This work was in part supported by NIH Laser Biomedical Research Center Grant #RR02594 and NSF Laser Research Center Grant #8619255-CHE. This work was also supported by Korean Science and Engineering Foundation under contract #913-0303-004-2.

References

1. Kittrell, C.; Willett, R. L.; de los Santos-Pacheo, C.; Ratliff, N. B.; Kramer, J. R.; Malk, E. G.; Feld, M. S. *Appl. Opt.* **1985**, *24*, 2280.
2. Richards-Kortum, R.; Rava, R. Cothren, R. P.; Mehta, A.; Fitzmaurice, M.; Ratliff, N. B.; Kramer, J. R.; Kittrell, C.; Feld, M. S. *Spectrochim. Acta.* **1989**, *45A*, 87.
3. Baraga, J. J.; Taroni, P.; Park, Y. D.; An, K.; Maestri, A.; Tong, L. L.; Rava, R. P.; Kittrell, C.; Dasari, R. R.;

Feld, M. S. *Spectrochim. Acta.* **1989**, *45A*, 96.
4. Alfano, R. R.; Tang, G. C.; Pradhan, A.; Lam, W.; Choy, D. S. J.; Opher, E. *IEEE J. Quantum Elec.* **1987**, *23*, 1806.
5. *Arterioisclerosis, Report of the working group on Arteriosclerosis of the National Heart, Lung and blood Institute*; DHHS-NIH Publication No. 81-2034: Washington, U. S. A., 1981; Vol. 1.
6. Braunwald, E., Ed.; *Heart Disease: A textbook of Cardiovascular Disease*; second ed.; W. B. Saunders Co., 1984.
7. *1989 Heart Facts*, American Heart Association, 1988.
8. Letokhov, V. S. *In Laser Picosecond Spectroscopy and Photochemistry of Biomolecules*; Letokhov, V. S., Ed.; Adam Hilger: Bristol, 1987; p 1-55.
9. Chang, M. C.; Petrich, J. W.; Mcdonald, D. B.; Fleming, G. R. *J. Am. Chem. Soc.* **1983**, *105*, 3819.
10. Hochstrasser, R. M.; Negus, D. K. *Proc. Natl. Acad. Sci. U. S. A.*, **1984**, *81*, 4339.
11. D. V. O'Connor and D. Phillips, Time-Correlated Single Photon Counting, Academic Press, Orlando, FL, U. S. A., 1984.
12. Fujimoto, D.; Akiba, K.-Y.; Nakamura, N. *Biochem. Biophys. Res. Commun.* **1977**, *76*, 1124.
13. Gallop, P. M., Blumenfeld, O.: Deifter, S. *Ann. Rev. Biochem.* **1972**, *41*, 618.

Studies of Nonstoichiometry and Physical Properties of the Perovskite $Sr_xHo_{1-x}FeO_{3-y}$ System

Kwang Sun Ryu, Sung Joo Lee, and Chul Hyun Yo

Department of Chemistry, Yonsei University, Seoul 120-749
Received November 8, 1993

Perovskite type oxides of the $Sr_xHo_{1-x}FeO_{3-y}$ system with compositions of $x=0.00$, 0.25, 0.50, 0.75, and 1.00 have been prepared at 1200℃ in air. X-ray powder diffraction assigns the compositions with $x=0.00$ and 0.25 to the orthorhombic crystal system and those with $x=0.50$, 0.75, and 1.00 to the cubic one. The unit cell volumes of solid solutions increase with x in the system. Nonstoichiometric chemical formulas were determined by Mohr salt titration. The mole ratio of Fe^{4+} ions to total iron ions and the concentration of oxygen ion vacancies increase with x. Mössbauer spectra for the compositions of $x=0.00$, 0.25, and 0.50 show six lines indicating the presence of Fe^{3+} ions in the octahedral site. However, the presence of Fe^{4+} ions may also be detected in the spectra for the compositions with $x=0.25$ and $x=0.50$. In the compositions with $x=0.75$ and 1.00, single line patterns show also the mixed valence state of Fe^{3+} and Fe^{4+} ions. The electrical conductivity in the temperature range of −100℃ to 100℃ under atmospheric air pressure increases sharply with x but the activation energy decreases with the mole ratio of Fe^{4+} ion. The conduction mechanism of the perovskite system seems to be hopping of the conduction electrons between the mixed valence iron ions.

Introduction

The atomic arrangement in the perovskite ABO_3 structure was first found for the mineral perovskite, $CaTiO_3$[1]. The unit cell of $CaTiO_3$ could be represented by calcium ions at the corners of a cube with titanium ions at the body center and oxygen ions at the center of the faces. In the perovskite structure, the A cation is coordinated with twelve oxygen ions and the B cation with six oxygen ions. Thus, the A cation is normally found to be somewhat larger than the B cation. In order to have contact between the A, B, and O ions, R_A+R_O should equal to $\sqrt{2}(R_B+R_O)$, where R_A, R_B, and R_O are the ionic radii.

The orthoferrites with the formulae $RFeO_3$, where R is a rare earth metal, have the space group $P_{bnm}(D_{2h})$. Their structure may be viewed as a distorted perovskite structure with four equivalent iron ions per unit cell. The Mössbauer spectra of various orthoferrites have been studied between room temperataure and the Néel temperature(T_N) by Eibschutz *et al.*[2], giving six-line spectra below T_N and single-line spectra above T_N. The Mössbauer spectra of the $SrFeO_x$[3]($x=$ 2.50, 2.60, 2.86, and 3.00) have been analyzed at 4°K, 78°K, and 300°K. Yamamura and Kiriyama[4] have studied the Mössbauer spectra and X-ray diffraction patterns of the $Sr_{1-x}La_xFeO_{2.5+x/2}$ system. Their results showed the existence of a five coordinated iron site surrounded by a trigonal bipyramid of oxygen at $0.2\leq x\leq 0.7$.

$LaFeO_3$ shows the orthorhombic crystal system with four $LaFeO_3$ perovskite units[5] and its neutron-diffraction spectra indicate that it has a G-type[6], spin-ordered antiferromagnetic structure below its Néel temperature of 750 K.

Mössbauer spectra of the $Sr_xDy_{1-x}FeO_{3-y}$ ferrite system have also been analyzed[7]. The Néel temperature of antiferromagnetic $LaFeO_3$ decreases with increasing Sr^{2+} ion concentration. Nonstoichiometric perovskite-related ferrites of composition $La_{1-x}Sr_xFe^{3+}_{1-\tau}Fe^{4+}\tau O_{3-y}$($0\leq x\leq 0.95$) have been studied by Wattiaux *et al*[8]. Due to the mixed valence state of Fe^{3+} and Fe^{4+} ions[9], the electrical conductivity of the perovskite annealed in oxygen is higher than that annealed *in vacuo*. Electrical conductivity of $LaFeO_3$ and $La_{1-x}Sr_xFeO_3$ ($x=0$. 1, 0.25) was studied by Mizusaki *et al*[10-11]. They found that the electronic conduction appeared to be *n*-type in the lower